Journal of Molecular Structure 1233 (2021) 130107

Contents lists available at ScienceDirect

Journal of Molecular Structure

journal homepage: www.elsevier.com/locate/molstr

New 2, 5-aromatic disubstituted pyrroles, prepared using diazonium salts procedures

Giovanna Angélica Vázquez-Hernández[a], Roxana Delgado-Cruz[a], María-Elena Sánchez-Vergara[b], Lioudmila Fomina[a], Virginia Gómez-Vidales[c], Beatriz de la Mora[d], Alonso Acosta[a], Citlalli Ríos[a], Roberto Salcedo[a,*]

[a] Instituto de Investigaciones en Materiales, Universidad Nacional Autónoma de México, circuito exterior s/n. Ciudad Universitaria, Coyoacán Ciudad de México 04510, México
[b] Engineering Department, Universidad Anáhuac México, Avenida Universidad Anáhuac 46, Col. Lomas Anáhuac, Huixquilucan, Estado de México, 52786, México
[c] Instituto de Química, Universidad Nacional Autónoma de México, Circuito Exterior s/n Circuito Exterior s/n, Ciudad Universitaria, Coyoacán Ciudad de México 04510, México
[d] Instituto de Ciencias Aplicadas y Tecnología. Universidad Nacional Autónoma de México, Circuito Exterior s/n Circuito Exterior s/n, Ciudad Universitaria, Coyoacán Ciudad de México 04510, México

ARTICLE INFO

Article history:
Received 14 November 2020
Revised 20 January 2021
Accepted 9 February 2021
Available online 15 February 2021

Keywords:
Fullerene
Organic semiconductor
Ferrocene
Diazonium salts

ABSTRACT

In this work, we have prepared new derivatives of the 2, 5 -aromatic disubstituted pyrrole. Fullerene and ferrocene were used as substituent fragments. These compounds are chemically different, however all of them withdraw electronic charge from the aromatic ring in which they are supported; as a result all the derivatives exhibit semiconductor behaviour. We describe the preparation of these species, and also characterize all of the new compounds. DFT calculations were carried out in order to establish the source of electronic behaviour and to make comparisons between the experimental results. The Kubelka-Munk method indicates that the fullerene compound is a low band gap semiconductor, thus we used this material to prepare thin films. The films were characterized and their optoelectronic behaviour was evaluated.

1. Introduction

Since the introduction of semiconductor substances as the main components of transistors in 1947 [1,2], a large variety of different substances with semiconductor behaviour have been studied from experimental and theoretical standpoints, in order to assess their propensity to work in transistors or similar devices. In 1950, Akamatu and Inokuchi made way for the introduction of organic semiconductor substances [3], by initiating a very interesting research project that had very fruitful results. Among these studies, research related to π-conjugated monomers and polymers stands out [4,5], which has provided fundamental materials for the design of devices, including photovoltaic cells [6], light emitting diodes [7,8] and transistors [9]. To date, polymer photovoltaic cells have undergone vast improvement, thanks to the photoconductivity in their polymers, furthering their future application in organic solar cells [10]. With reference to their chemical qualities, there are four groups of photoconductive polymers [10,11]: (i) polymers with a saturated backbone, (ii) polymers with polynuclear aromatic moieties, (iii) polymers with a high degree of π-conjugation in the main chain and (iv) polymers with a σ-conjugated backbone [10,12].

Pyrrole is a heterocyclic compound with a high degree of π-conjugation in the main chain, which has manifested semiconductor behaviour [13] and been probed as a corner stone for the design of materials with interesting electronic properties [14]. In particular, 2, 5 -aromatic disubstituted derivatives of pyrrole [15,16] show electronic tuning behaviour, and it has been demonstrated that the introduction of different substituent groups on the aromatic, dramatically changes its behaviour from insulator to semiconductor, resulting in better semiconductor capacity when the functional groups participate in an electron release, consisting of $-NO_2$ [17,18]. Moreover, the diketopyrrolopyrrole (DPP) acceptor unit has recently emerged as a promising candidate for use in optoelectronic applications [10,19,20]. For example, the PDPP3T was designed with unsubstituted terthiophene units between each pair of DPP units, and has exhibited not only high charge carrier mobili-

* Corresponding author.
E-mail address: salcevitch@gmail.com (R. Salcedo).

https://doi.org/10.1016/j.molstruc.2021.130107
0022-2860/

ties of around 10^{-2} $cm^2V^{-1}s^{-1}$ for electrons and holes, but also extended optical absorption towards the infrared region, with a low band gap of 1.36 eV [10]. Most recently, furans have been incorporated into DPP acceptor units to produce a low-band gap of between 1.35 and 1.41 eV, in these conjugated polymers [10].

A diazonium salt is an ionic unstable organic species, which bears a triple-bonded di-nitrogen unit [21]. Above all, aryl diazonium salts constitute an important series of compounds that are commonly used in organic chemistry because the diazonium group activates nucleophilic aromatic substitutions and provides a routine way for introducing a wide range of compounds, as well as the fact it can be easily synthesised, manifests rapid electron-reduction and strong aryl-surface covalent bonding [22]. It can be prepared from aniline or an aromatic species bearing $–NH_2$ substituents, which can be obtained from the reduction of the corresponding nitroarene [23].This type of chemistry has been successfully applied to various processes for the functionalization of materials, for example the modification of carbon surfaces via grafting of electrochemically reduced aryl diazonium salts [24,25], covalent functionalization of CNO's [26], SWCNT's [27], semiconductors, fullerene and metal-oxide nanoparticles [26–28]. Considering that the conductivity of pyrrole derivatives can be improved by the inclusion of new electron withdrawing groups into the N- substituted aromatic ring of the framework species, the diazonium salts method may offer an interesting alternative for the preparation of new substances. In this case, the introduction of organic and organometallic compounds such as ferrocene and fullerene to the pyrrole unit may generate an interesting group of semiconductor compounds, due to favourable physical, chemical and electronic properties. Ferrocene (Fc) is one of the most widely used organometallic molecules in functional materials for sensors [29], solar cells [30], magnets [31], and biological applications [32,33]. Chemically, Fc groups have unique redox characteristics and a pi-conjugated system, which potentially offer superb electron-transfer capacity. In another context, fullerene has attracted interest due to its highly symmetric structure, its ability to undergo multiple addition reactions and its exceptional electron accepting characteristics. With its strong electron accepting properties and remarkably low reorganization energy, C_{60} is one of the most popular chromophores to have been incorporated into multicomponent molecular architecture [34].

This work therefore aims to prepare new derivatives of 2, 5-aromatic disubstituted pyrroles, functionalized with fullerene and ferrocene, by applying the diazonium salts procedure. Subsequently, we implemented chemical and structural characterization of these pyrrole derivatives. Finally, their optoelectronic nature was evaluated, applying a thin film analysis, in the case of the fullerene derivative. DFT calculations were undertaken, in order to establish the source of electronic behaviour and then compared with experimental results and in the case of ferrocene derivatives calculations of the same nature were carried out in order to compare the intrinsic electronic differences between both isomers.

2. Materials and methods

2.1. Synthesis of precursor compounds

Reagents and solvents employed in all syntheses were purchased from Sigma-Aldrich Chemistry. The preparation of these precursor compounds has been reported previously [15,18].

1, 4-diphenylbuta-1, 3-diyne (I). We added copper (I) chloride (0.9 g, 9.09 mmol) and N, N, N′, N′-tetramethylethylenediamine (TMEDA), 0.3 mL (0.23 g, 1.99 mmol) to a solution of phenyl acetylene (4.65 g, 45.53 mmol) in isopropanol. The mixture was stirred continuously for 3 hours in an oxygen atmosphere. Acidified water was added to the resulting solution. The product was separated by filtration, dried in a vacuum, and purified by recrystallization from hexane. Yield: 95%, white solid, m.p. 86.5°C.

IR (cm^{-1}): ν(C-H): 3049, ν (C≡C): 2146, ν(C=C): 1592, ν(C-H): 1438 y 1484.

^{1}H-NMR (400 MHz, $CDCl_3$): δ (ppm) 7.71 (s, 2H), 7.53 (m, 3H).

^{13}C-NMR (100MHz, $CDCl_3$): δ (ppm) 73.92, 81.55, 121.81, 128.43, 129.19, 132.49.

1- (p-nitro-phenyl) -2, 5-diphenylpyrrole (II). We added CuCl (I) (0.2g, 1.97mmol) and 4 -nitroaniline 1.36 g (9.84 mmol) to a solution of 1, 4-diphenylbuta-1, 3-diyne (2g, 9.8mmol) in N, N-dimethylformamide (DMF) (15mL). The reaction mixture was then stirred constantly for 48 hours in a nitrogen atmosphere, at a temperature of 153°C. Subsequently, this product was washed several times in cold acetone, separated by filtration and dried in a vacuum. Yield: 50%, yellow solid, m.p. 253-255°C.

IR (cm^{-1}): ν (C-H):3063, (-NO_2): 1521, 1496, (C-H): 1677, 1595, (-NO_2): 857.

^{1}H-NMR (400 MHz, $CDCl_3$): δ (ppm) 6.65 (s, 1H), 7.27 (m), 8.23 (s, 1H).

^{13}C-NMR (100 MHz, $CDCl_3$): δ (ppm) 111.26, 132.52, 135.72, 128.26, 128.97, 129.31, 144.50, 126.95, 124.10 y 146.07.

Synthesis of 1- (p-amino-phenyl) -2, 5-diphenylpyrrole (III). 0.5 g (1.47 mmol) of 1- (p-nitro-phenyl) -2, 5-diphenylpyrrole in 75 mL of ethyl acetate was placed in a three-necked flask, and stirred constantly for 10 min at 60°C. Then we added 0.6 g (10.74 mmol) of metallic Fe and 5 mL of concentrated HCl. The mixture was stirred constantly for 3.5 h at reflux in a nitrogen atmosphere, at 75°C. When synthesis was complete, the reaction mixture was filtered in a vacuum and the extracted solid was washed several times with distilled water and the product dissolved in acetone. The product solution was concentrated in the rotavapor. Yield: 70%, caramel brown solid, m.p. 240.42°C.

IR (cm^{-1}): ν (N-H):3413 y 3331, ν (C-H): 3061, ν (N-H): 1623 y 1597, ν (-C-H): 1513 and 1482.

^{1}H-NMR (400 MHz, $CDCl_3$): δ (ppm) 6.42 (s, 1H), 6.74 (s, 1H), 7.16 (m, 3H), 5.58 and 6.60 (d, 1H), 4.22 (s, 1H).

^{13}C-NMR (100 MHz, C_2D_6OS): δ (ppm) 110.13, 128.7, 130.28, 128.50, 128.60, 128.78, 133.40, 127.31, 126.71, 136.11.

Synthesis of ferrocene derivatives (IV, V). 0.093 g (0.3 mmol) of 1- (p-amino-phenyl) -2, 5 - diphenylpyrrole was placed in a ball-flask (1) with 10 mL of concentrated H_2SO_4, then stirred for 20 min in another ball flask, in which (2) 0.06 g (0.32 mmol) of ferrocene was placed in 10 mL of ether and stirred constantly for 10 min. A solution of 0.28 g of $NaNO_2$ (4 mmol) with 5 mL of H_2O was stirred continuously for 10 min. The solution in the ball flask (1) and the $NaNO_2$ solution were added dropwise to the ball flask (2). The reaction mixture was kept for 3 h, stirring continuously at room temperature. The mixture was then washed with distilled water. Subsequently, the reaction mixture was washed with chloroform and another solid and the solution was retrieved. The part dissolved in chloroform was transferred to the rotavapor, obtaining a dark brown compound **IV**, with a yield of 41.97%. Solid compound **V** was light brown in colour, with a yield of 23.67%.

IR of compound **IV** (cm^{-1}): ν (C-H): 3050 y 2917, ν (-C=C): 1677, ν (Fe-Cp): 593, ν (-C-H): 1596 and 1494.

^{1}H-NMR (400 MHz, $CDCl_3$): δ (ppm) 6.93 (s, 1H), 0.90 (s, 1H), 1.28 (s, 3H), 7.56 (m, 5H).

^{13}C-NMR (100 MHz, $CDCl_3$): δ (ppm) 110.23, 88.25, 57.21, 29.71, 128.94, 136.90, 133.92, 128.94.

IR of compound **V** (cm^{-1}): ν (C-H): 3060, ν(C=C): 1514, ν (C-C): 1483 and 1598, ν (-C-H): 1040, ν (Fe-Cp): 588, (Fe-C): 401.

Synthesis of 1- (p-fullerene-phenyl) -2, 5 - diphenylpyrrole (VI). We placed 0.09 g (0.290 mmol) of 1- (p-amino-phenyl) -2, 5-diphenylpyrrole with 3 mL of concentrated HCl in a ball flask and stirred for 2 h. A solution of $NaNO_2$ (0.03 g, 0.434 mmol) in 2 mL of H_2O was prepared. The ball flask solution and the $NaNO_2$ solu-

tion were cooled to 0°C. Once this temperature was reached, 0.1 g of fullerene (0.138 mmol) and the $NaNO_2$ solution were added to the mixture in the ball flask. The reaction mixture was stirred continuously for 15 days, at room temperature. Yield: 57.89%, dark brown solid, m.p. 205.23 °C.

IR (cm^{-1}): ν (C-H): 3056, ν (C-H): 1513 y 1483, C_{60}: 1427, 1180, 574 y 524.

^{13}C-RMN (400MHz, solid): δ (ppm) 148.01, 135.49, 118.50, 127.99, 129.53, 110.17 and 78.58.

2.2. Pyrrole derivative characterization

Infrared spectra were recorded on a Thermo Scientific model Nicolet 6700 FT-IR spectrometer. ^{1}H and ^{13}C NMR spectra were obtained using the Bruker Avance 400 MHz spectrometer, with TMS as standard. TGA thermal analyzes were performed on a TA Instruments Q5000IR in an air atmosphere with a flow of 25 mL min^{-1} and a heating rate of 10°C min^{-1}. DSC analyzes were performed on a TA Instruments Q2000 in an N_2 atmosphere with a flow of 50 mL min^{-1} and a heating rate of 10°C min^{-1}. UV-vis spectroscopy was carried out on a spectrophotometer Unicam UV-300, at a wavelength range of 200-1100 nm.

For ferrocene compounds, electronic paramagnetic spectroscopy (EPR) was undertaken in a quartz tube at room temperature with a Jeol JES-TE300 spectrometer, operating at X-Band fashions at 100 kHz modulation frequency and a cylindrical cavity in the TE_{011} mode. The external calibration of the magnetic field was made using a precision gaussmeter, Jeol ES-FC5. These values were corrected by isotropic simulation using the ES-PRITS/TE programme from Jeol.

The diffuse reflectance of the samples of ferrocene and fullerene derivatives were measured in powder form at 25°C using a UV-Vis NIR Cary 5000 spectrophotometer, at a wavelength ranging from 200-800nm. We used the Kubelka-Munk method to obtain band gap energies.

Tauc's theory [35] proposes a method to estimate the band gap energy of amorphous semiconductors using the optical absorption spectrum, based on the assumption that the absorption coefficient α can be expressed according to the following Eq. (1):

$$(\alpha \cdot h\nu)^{1/\gamma} = B(h\nu - E_g) \tag{1}$$

Where $h\nu$ is the energy of the incident photon, E_g is the optical band gap energy, and B is a constant. The γ factor depends on the nature of the electron transition, which is equal to $\frac{1}{2}$ or 2 for direct and indirect band gap energy transitions, respectively. It has been proved that when properly executed; this method provides accurate values for E_g. However, because α is used to construct the Tauc plot, negligible light scattering is required for this method to function successfully. In the case of powder samples, the scattering component cannot be ignored; thus optical absorption spectroscopy does not constitute an appropiate technique for determining the value of E_g. In this case, diffuse reflectance spectroscopy offers a better method for analysing band-gap energies.

The parameters necessary for implementing the graphical method are obtained by analysing the results deduced from diffuse reflectance, using the Kubelka-Munk equation [36]. This makes it possible to convert the reflectance measured in experiments, into values for the absorption coefficient α, so that they can subsequently be plotted, thus reveal the band gap value. Firstly, it is necessary to calculate the Kubelka-Munk or reemission function F (R_∞), analogous to Tauc's plots (see Eq. 2):

$$F(R_\infty) = \frac{K}{S} = \frac{(1 - R_\infty)^2}{2R_\infty} \tag{2}$$

Where $R_\infty = \frac{R_{sample}}{R_{standard}}$ is the reflectance from an infinitely thick specimen, and K and S represent absorption and scattering coefficients, respectively. Finally, putting F (R_∞) instead of α into Eq. 1 yields the form (Eq. 3) [37,38]:

$$(F(R_\infty) \cdot h\nu)^{1/\gamma} = B(h\nu - E_g) \tag{3}$$

2.3. Geometry optimization

Geometry optimizations were obtained using the DFT method based on a combination of Becke's gradient corrections [39] for exchange and Perdew-Wang's for correlation [40]. This is the scheme for the B3PW91 method, which is included in the GAUSSIAN16 package [41]. These calculations were performed using the 6-31 G** basis set.

2.4. Deposition and characterization of thin films

The powder obtained from the fullerene compound was deposited in the form of thin films on different substrates, in a high vacuum chamber, using the sublimation technique. The substrates used were: PET coated with an indium tin oxide film (ITO), monocrystalline silicon wafers type "n" (c-Si) and glass. The silicon and glass substrates were previously washed, employing an ultrasonic bath cleaning process with different solvents and then vacuum dried. Subsequently, to effect the deposition, the substrates were placed on a stainless-steel base inside the vacuum chamber at approximately 8 cm above the crucible, where evaporation was carried out. The powders of the synthesized material were placed on a molybdenum crucible at room temperature. When the heating process was initiated, the temperature reached within the chamber was approximately 573 K. The deposition rate was 0.2 Å / s and the pressure in the vacuum chamber was 10^{-6} torr.

Infrared analysis was carried out for the films deposited on the silicon wafers. IR spectroscopy was performed on a Thermo Scientific Nicolet iS5 FT-IR spectrometer. Optical absorption studies of films deposited on quartz substrates were measured on a Thermo Scientific Evolution 220 UV-Vis spectrophotometer, at a wavelength ranging from 200-1100 nm. X-ray diffraction patterns were obtained from the films deposited on the glass and silicon wafer substrate with CuKα radiation (λ = 1.54183 Å) in a Bruker-D8 Advance diffractometer. Measurements were made in grazing beam mode at 1 ° inclination on the sample, with a measurement interval of 2 °-60 °, a step size of 0.02 ° and a step time = 1.5 s. SEM images were obtained on a SEM JEOL 7600 scanning electron microscope, operated at a voltage of 20 kV, using the films deposited on glass and silicon. For the electrical **characterization** of the devices made on PET-ITO films, we used a programmable voltage source; a sensing station with a lighting and temperature controller circuit from Next Robotix and auto-ranging Keithley 4200-SCS-PK1 picoammeter analyser.

3. Results and discussion

3.1. Synthesis and characterization of precursor compounds

The preparation of **1, 4- diphenylbuta-1, 3- dyine (I)** was carried out based on the Glaser reaction, which includes the Hay modification. This method consists of the oxidative coupling of terminal alkyne groups, employing a catalyst of copper chloride, and isopropanol as solvent [42,43].

The trisubstituted pyrrole **(II)** compound was prepared by means of the Reisch and Schulte reaction [44–46]. During this procedure, the 4-nitroaniline, containing an electron withdrawing group (-NO_2) reacts in the presence of copper chloride at 153°C in DMF and N_2 atmosphere for a 48 h period. The use of polar solvents as DMF favors the formation of pyrroles [47]. The IR spectrum corresponding to compound **II** manifests the characteristic

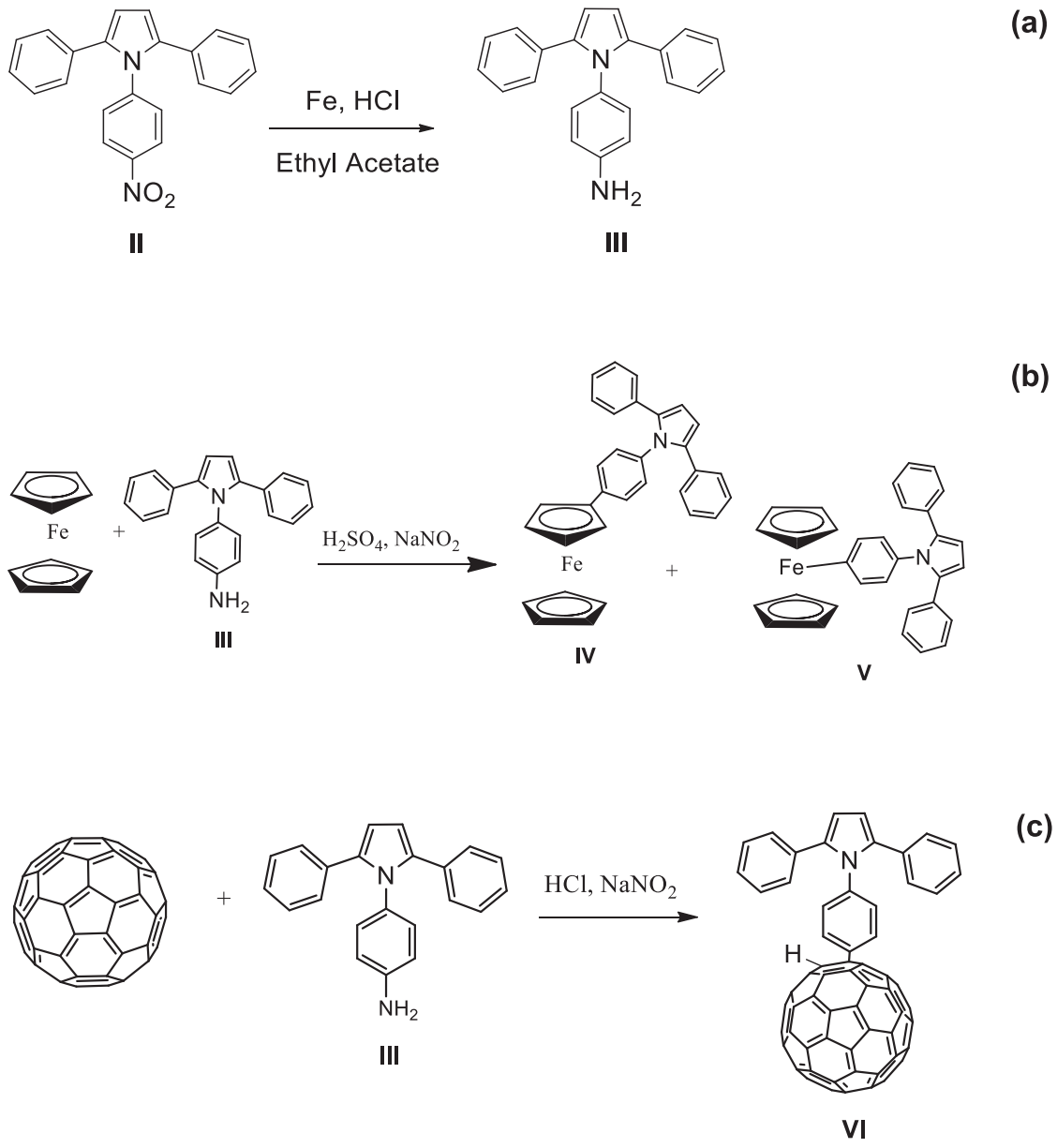

Scheme 1. Chemical reactions: (a) Reduction of the NO_2 group to NH_2, (b) Formation of ferrocene derivatives, (c) Formation of 1-(p-fullerene-phenyl)-2,5-diphenylpyrrole.

adsorption band at 3063 cm $^{-1}$ pertaining to the (C-H) group vibrations, as well as the symmetric and asymmetric vibrations from the NO_2 group at 1521 and 1496 cm^{-1}. The ^{1}H NMR **spectrum** from this same compound shows a singlet signal at 6.65 ppm, which corresponds to the two hydrogen atoms supported on the pyrrole ring, a fact confirming that this ring was formed in the reaction. The signals of 73.99 and 81.61 ppm from the ^{13}C spectrum, which belong to the acetylenic groups, disappear after the reaction, whereas the signal at 111.26 ppm, corresponding to the 2, 5-disubstituted pyrrole group, appears after the reaction.

3.2. Synthesis and characterization of compound 1-(p-amino-phenyl)-2, 5-diphenylpyrrole

1-(p-amino-phenyl)-2, 5-diphenylpyrrole (III), was prepared following the Béchamp method [48], which consists of the reduction of nitro groups to the corresponding amine species. The catalyst is iron powder and a Brönsted acid is added in order to increase the yield from the reaction (see Scheme 1a). In this reaction, aromatic nitro compound is adsorbed onto the iron surface. Here, it reacts with hydrogen ion H^+ produced from the water and acid reaction, which generates the production of amine [49] and the concentration of this acid rules this electronic transfer, because its excess helps it pass through the reaction determining step, leading to the formation of -NH_2 [50]. The FT-IR analysis shows the apparition of typical absorption bands at 3413 and 3331 cm^{-1}, corresponding to the symmetric and asymmetric vibrations from the amine group, besides the bending vibration from this same group at 1623 cm^{-1} and the disappearance of the nitro group band of 1521 cm^{-1}; a set of signals which confirms the formation of the desired compound in pure form. The NMR analysis makes it possible to observe the 6.42 ppm peak from the pyrrole ring and the 4.22 ppm peak from the hydrogen atoms of amine in the ^{1}H spectra. Furthermore, the 110.13 ppm signal from the pyrrole group and the 136.11 ppm signal from the carbon atom joined to the amine group, appear in the ^{13}C spectrum.

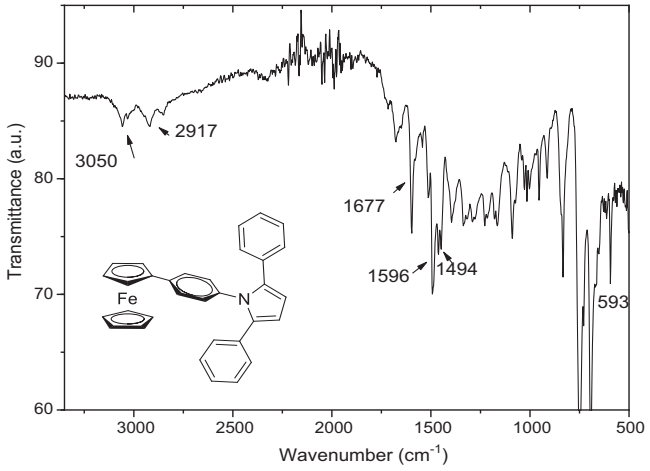

Fig. 1. IR spectrum of 1-(p-ferrocene-phenyl)-2, 5- diphenylpyrrole (IV).

3.3. Synthesis and characterization of the ferrocene derivatives (IV, V)

The preparation of **1-(p-ferrocene-phenyl)-2, 5-diphenylpyrrole (IV)** was carried out, following the diazonium salts procedure, which consists of the formation of the cationic species R-N_2^+ and the posterior formation of an N_2 molecule. The reported method of preparation [51] was modified using H_2SO_4 instead of HCl in order to improve solubility of the reactant substance 1-(p-amino-phenyl)-2, 5-diphenylpyrrole, in the sulfuric acid (see Scheme 1b). The reactant mixture was washed with distilled water, and the resulting solid was put in chloroform, yielding two phases; one soluble **(IV)** and one insoluble **(V),** in this solvent.

Analysis of compound **IV** includes the experimental FT-IR, which was compared to the theoretical one, a comparison which was undertaken from 400 to 3700 cm^{-1}, for which the following bands match well, with a tolerance of 5 cm^{-1}; those corresponding to the (C-H) group at 3050 and 2917 cm^{-1}, on the theoretical spectrum 3292 y 3220 cm^{-1}, and those belonging to the (C=C) group at 1677 cm^{-1} (theoretical: 1676 cm^{-1}). The **bands** at 1596 and 1494 cm^{-1} **correspond** to the ν(-C-H) group (theoretical values: 1596 and 1588 cm^{-1}) and the one at 593 cm^{-1} corresponds to the stretching of the FeCp group (theoretical: 628 cm^{-1}). The amine bands do not appear; confirming that the compound is pure (see Fig. 1). The same analysis for compound **V** shows almost the same bands that appear in compound **IV**, here again the band at 588 cm^{-1} is evident, corresponding to the Fe-C bond of the cyclopentadienyl ring (see Fig. 2a). However, there is a new band at 401 cm^{-1} which corresponds to an Fe-C σ bond, indicating that in this isomer, the bond between the metal atom and the benzene ring is σ (see Fig. 2b).

In Fig. 3, the ^{1}H-NMR spectrum of compound **IV** is shown. The signals corresponding to the proton atoms of pyrrole are visible, with chemical shifts of 6.93 ppm (H-1) (theoretical 6.89); 0.90 ppm (H-7) (theoretical 0.88) and 1.28 ppm (H-8, H-9, H-10) (theoretical 1.25), corresponding to the protons of the ferrocene cyclopentadiene. Aromatic proton atoms found in a multiplet centred at 7.56 ppm (H-2, H-3, H-4, H-5, and H-6) (theoretical 7.52).

Compound **V** is paramagnetic, with an unpaired electron; this is demonstrated by the corresponding ^{1}H-NMR spectrum (Fig. 4a) and EPR spectrum, shown in Fig. 4b. Results from this study confirm this electronic behaviour. As ferrocene is a silent epr compound, given the oxidation state of iron Fe^{+2}, the appearance of an isotropic broad signal in the EPR spectrum in the central field with g=20019 and ΔH_{pp} = 10 mT, suggests the oxidation of a part

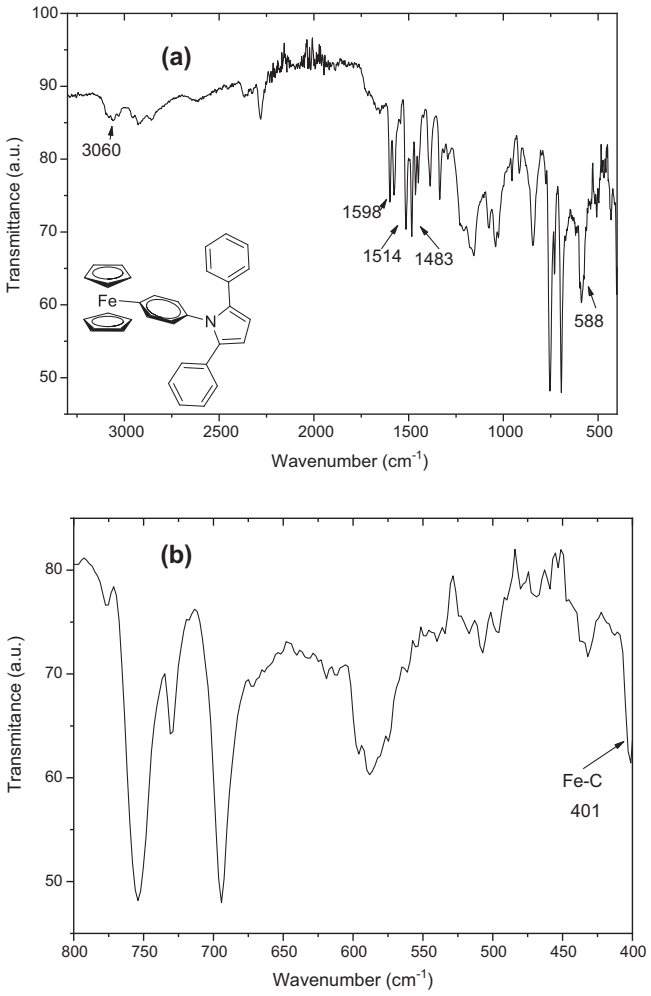

Fig. 2. (a) IR spectrum of compound V. (b) Amplification of the area where the Fe-C bond band is at 401 cm^{-1}.

of the sample at Fe^{+3}, in low spin S=1/2. Overlapping with this signal assigned to Fe^{+3}, another very narrow signal was detected, also isotropic in character with g=2.0019 and ΔH_{pp} = 0.38 mT; it does not present hyperfine coupling, so due to its characteristics, the presence of an organic radical was assumed. The oxidation state of iron changes from 2+ to 3+; a state which characteristically appears in the EPR spectrum, meaning that this is a free radical species; it also manifests a very uncommon σ Fe-C bond [52–54].

The DSC study shows an exothermic peak at 127.6°C, an energy release which can possibly be explained in two ways. Firstly, this may be crystallization energy or the broken of energy from the σ; the fact that the compound does not manifest fusion temperature would seem to suggest that the second possibility is correct.

4. Synthesis and characterization of compound 1-(p-fullerene-phenyl)-2, 5-diphenylpyrrole (VI)

Organo-fullerene compounds are not common species because direct reactions between a fullerene species and organic compounds have seldom been witnessed [55]. Known reactions for this feature entail the rupture of the double bond at the surface of the fullerene cage and the substitution of a functional group and a hydrogen in that position, employing the mecha-

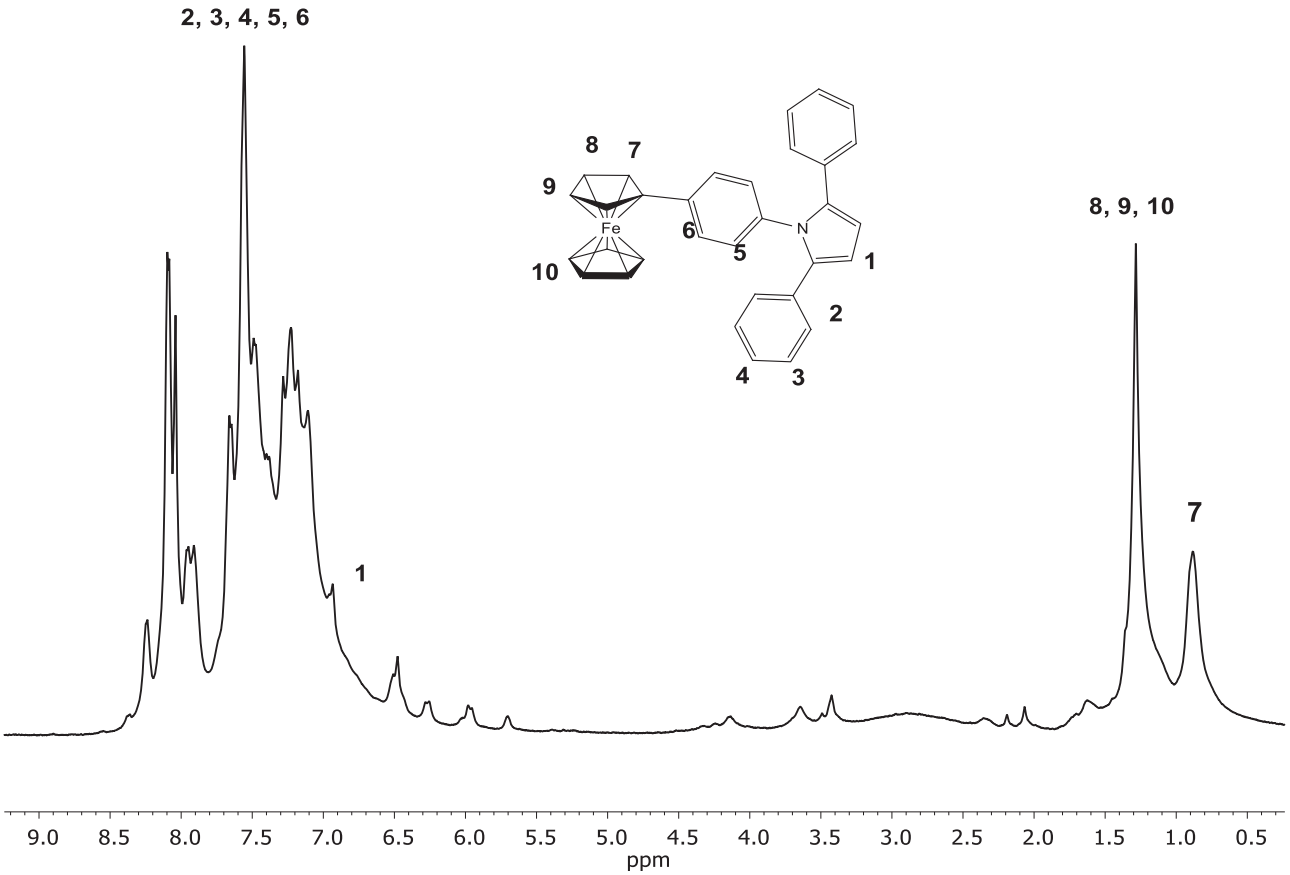

Fig. 3. ^{1}H-NMR spectrum of compound IV in $CDCl_3$.

nism for aromatic electrophilic substitution [56,57]. The synthesis of compound **VI** was also carried out by means of a diazonium salts reaction, related to the signalling mechanism. In this case, the HCl environment was used to search for the generation of nitrous acid and the generation of the diazonium ion at 0°C (this low temperature was necessary because of the poor stability of this reaction, when aromatic amines are involved). After the addition of $NaNO_2$ and fullerene (C_{60}), the mix was stirred for 15 days at room temperature, yielding 57.89%; the resultant powder was dark brown in colour and stable in air and light (see Scheme 1c).

In the FT-IR spectra for this species the absorption bands corresponding to the amino group on 3413 and 3331 cm^{-1} disappear (see Fig. 5a) and the pyrrole characteristic band of 3056 cm^{-1} is visible, as well as those at 1427, 1180, 574 and 524 cm^{-1}, which are attributed to the C-C and C=C bonds on fullerene, (see Fig. 5b) [58,59]. The NMR study (see Fig. 6) was carried out on solid state because of the strong insolubility of compound **VI**. The signal on 110.17 ppm from the ^{13}C spectrum can be attributed to the pyrrole fragment, whereas the 135.49 and 148.01 ppm correspond to the sp^2 carbon atoms from fullerene and the 78.58 ppm to the sp^3 carbon atoms [60,61].

All these results show that the diazonium salts methodology can act as a useful and versatile method for functionalizing species, which are not commonly structurally modified. This approach offers several ways to search for interesting derivatives of metallocene substances, in which even the metal centre can participate in novel bonding. Besides, the fullerene cages can find an alternative strategy for producing different classes of decorates, leading to some useful new materials.

4.1. Band gap values

The E_g band gap of paramagnetic ferrocene and fullerene derivative (samples **V** and **VI**) was calculated using the Kubelka-Munk method, with Eq. (3). The $(F(R_\infty)\cdot h\nu)^2$ vs $h\nu$ graphs were plotted. In the graphs, a straight line is fitted to the straight segment. The extrapolation of this straight line to the axis $h\nu$ indicates the band gap value for compound **V**, which was 2.01 eV. For compound **VI**, apparently two types of transitions occur: the first transition in 1.75 eV corresponds to the onset of optical absorption and the second transition in 1.86 eV is the fundamental energy gap (see Fig. 7). From the previous results, it is apparent that the presence of fullerene in compound **VI**, in addition to enhancing its charge carrying capacity, generates a material with a low band gap [10]. Therefore, it is apt for use as a component in optoelectronic devices. Apparently, the frontier energy levels of the fullerene are aligned, so that efficient electron transfer is achieved, when paired with polymer electron donors [62,63]. Likewise, the fullerene derivative has low reorganization energies upon electron transfer [62,64]. This derivative can be utilized in polymer photovoltaic devices, due to the light absorption caused by its reduced symmetry, which results in the lower-energy transitions of the fullerene derivative [62,65]. To determine its possible function in optoelectronic devices, an analysis of its properties must be carried out on thin films of this material.

4.2. Thin films: structure, morphology, and properties

Thin films were prepared from compound **VI**, and retrieved by means of the low pressure sublimation process, a technique which

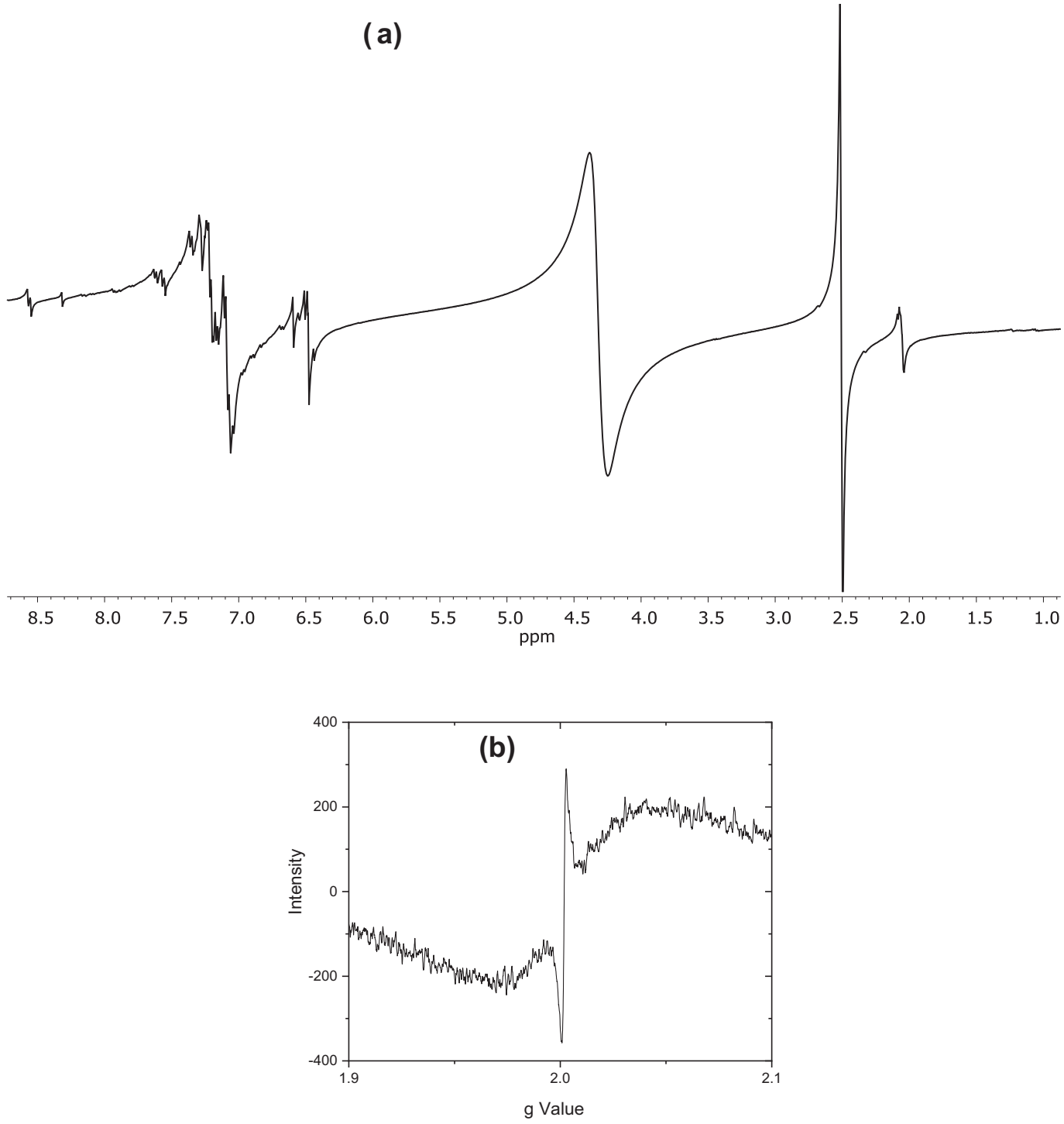

Fig. 4. (a) ^{1}H-NMR spectrum of compound V in DMSO-d_6, (b) EPR graphic of the behaviour of V.

was chosen because of the high quality and uniformity of the resulting surfaces. It is also important to consider the thermal stability of the film during the vaporization under low pressure, bearing in mind its possible application for optoelectronic devices. An FT-IR analysis was carried out after the deposition procedure in order to ensure the preservation of the integrity of the compound. The characteristic bands in the film closely match the spectrum of the KBr pellet: the pyrrole band at 3055 cm^{-1} as well the bands at 1428, 1182, 575 and 525 cm^{-1}, which can be attributed to the bonds on fullerene.

The crystallinity of the sample was studied because this feature can have compelling influence in terms of promoting electronic transport through frontier molecular orbitals (HOMO-LUMO gap). The x-ray diffractogram, corresponding to the thin film from compound **VI**, deposited on a substrate of monocrystalline silicon, is shown in Fig. 8. The fact that diffraction peaks are well defined is very significant as this may indicate that the sample is polycrystalline, meaning that electronic transitions will be well defined. The signals correspond to a cubic phase centred on the faces, which is characteristic of C_{60}; the set of peaks observed at $2\theta =$

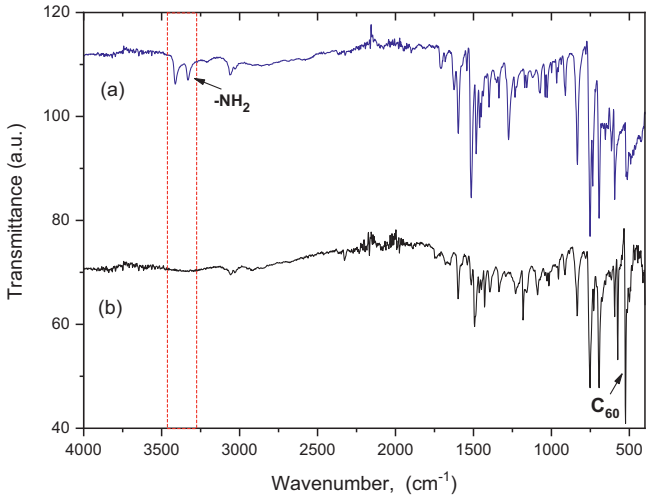

Fig. 5. Comparison of IR spectra of (a) 1-(p-amino-phenyl)-2, 5-diphenylpyrrole and (b) 1-(p-fullerene-phenyl)-2, 5-diphenylpyrrole.

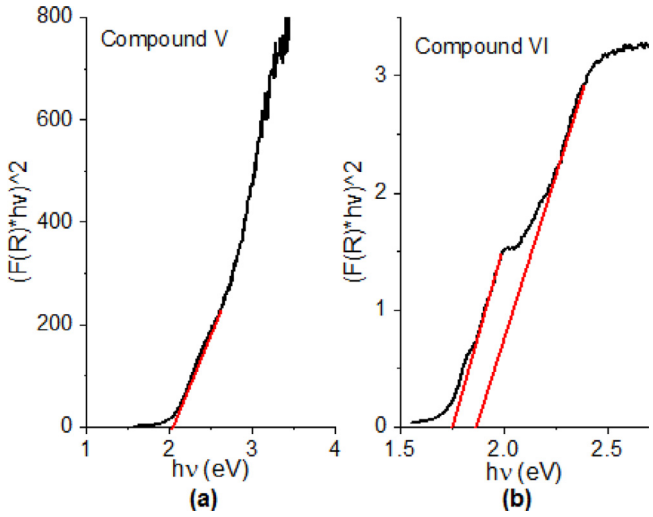

Fig. 7. (E_g) band gap energies of (a) Compound V and (b) Compound VI.

10.76°, 17.742°, 20.815°, 28.168°, 30.956° and 32.994° correspond to the reflection planes in the directions (111), (220), (311), (331), (422) and (511), respectively [66,67]. The study of morphology and uniformity was achieved using the SEM technique. Fig. 9 shows the SEM micrographs of the thin film deposited on silicon wafers with amplifications of 5000x, 25000x and 50000x. Fig. 9a shows the uniformity of the surface with homogeneous distribution over the base. There are no holes or particle clusters. Fig. 9b shows the magnification at 25000x and the granular nature of the surface is highlighted, also revealing small caves among the grains, whereas the 50000x amplifications (Fig. 9c) show the rough texture of these grains. This morphology is the result of the film growing process, which initially reacts to high temperatures, with a subsequent gradual lowering of these values, favouring the formation of grains on the surface. These attributes strongly suggest good electronic characteristics.

Transmittance T (λ) measured, at a wavelength range of 200-1000 nm for the compound **VI** film deposited on glass substrate, is shown in Fig. 10a. Apparently at shorter wavelengths (λ<500 nm), the film becomes nearly transparent. At longer wavelengths, λ>500 nm, the film presents transmission. The film shows increased transmittance in the visible region from 500 to 700 nm and from 700 nm it begins to oscillate between 70 and 83% transmittance. The absorbance of fullerene derivative is enhanced slightly and shows two weak red-shifted peaks at 864 and 960 nm, possibly considered a characteristic property of fullerene derivatives [68]. This further indicates the successful connection of the pyrrole moiety to the fullerene [68].

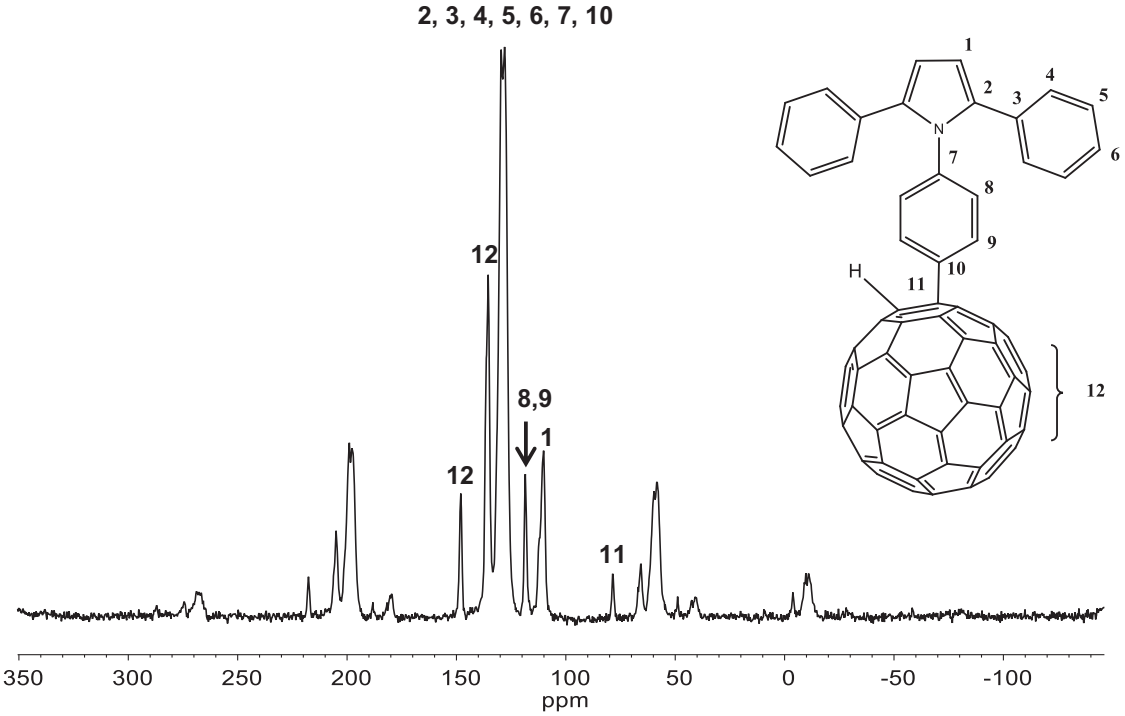

Fig. 6. ^{13}C-NMR spectrum of compound VI in solid.

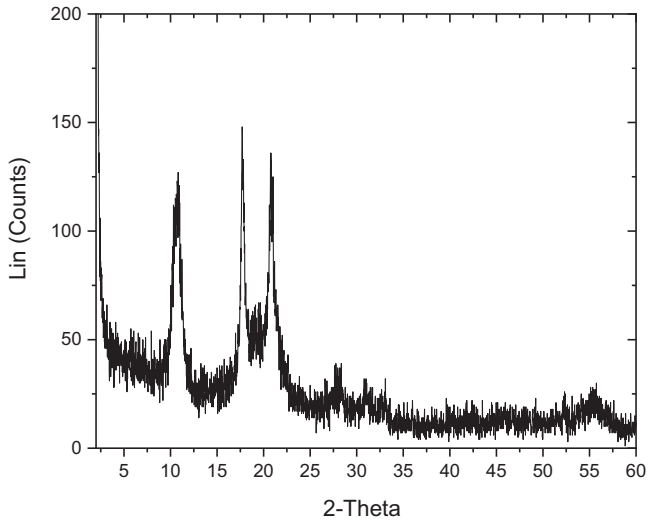

Fig. 8. Difractogram of thin film of compound VI.

Finally, the film of compound **VI** was evaluated in terms of its electrical behaviour and the results are shown in Fig. 10b. To carry out measurements of electrical current-voltage (I-V), the film was deposited on a glass substrate, using ITO (indium tin oxide) and silver as electrodes. According to the I-V graph, the film exhibits symmetrical behaviour, as a result of the ambipolarity of compound **VI**. Reversing the polarity of the electrodes does not result in rectification of the current, thus indicating that there is good energetic correlation between the work function of the electrodes (ϕ_{ITO} = 4.7eV; ϕ_{Ag} = 4.2eV) and the energetic level of the fullerene derivative (HOMO = -5.45 eV and LUMO= -3.29 eV) that participates in charge transport (see energetic diagram in Fig. 10b). There is evident ohmic-like behaviour. Electric charges flow along the film with no barriers between the electrode-thin film interfaces. This ohmic behavior and the value of the band gap are an indication of the semiconductor character of compound **VI**, demonstrating the possibility of using it in optoelectronic devices; probably as a resistor.

5. Theoretical results

The optimized geometries of the three compounds under study are shown in Figs. 11 and 12:

The most important comparison of these results with the experimental ones involves the HOMO-LUMO energy gap of the described species, the results are the next:

In the case of the ferrocene derivatives it is found a good matching, compound **V** which is an open shell species yields a re-

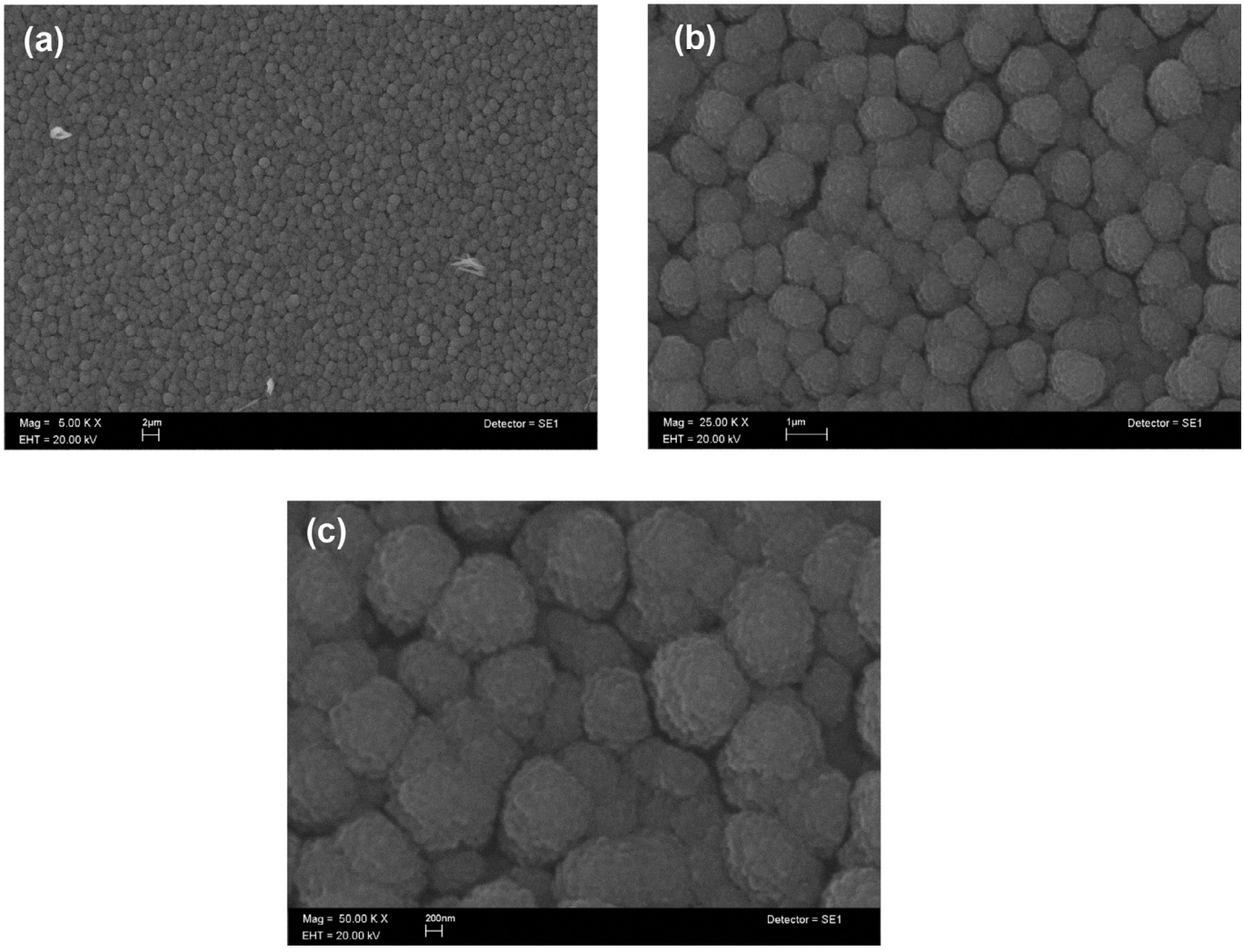

Fig. 9. SEM micrographs taken of thin film of compound VI at different amplifications: (a) 5000x, (b) 25000x and (c) 50000x.

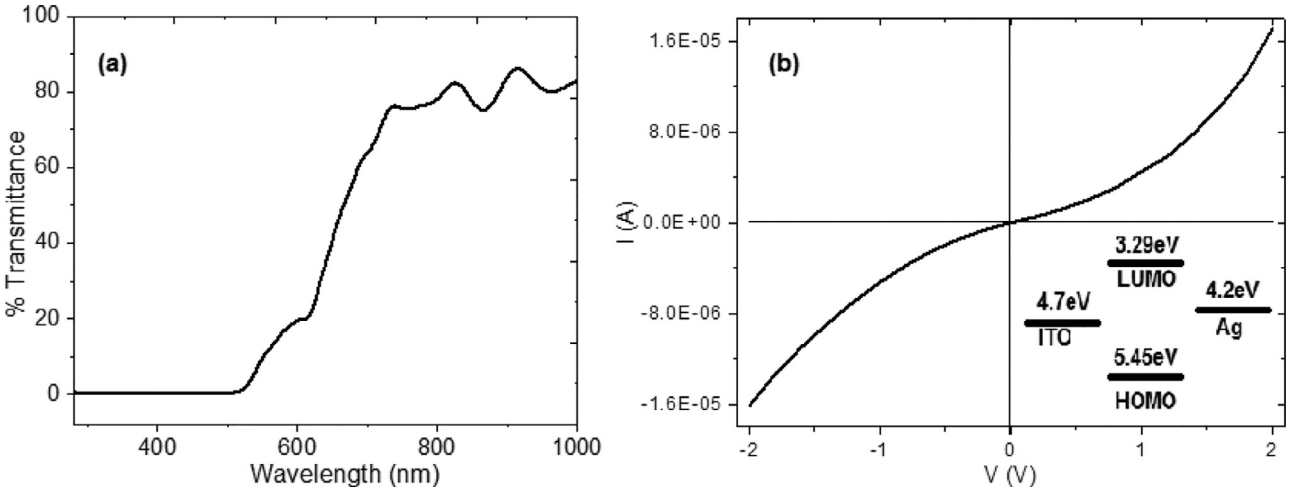

Fig. 10. (a) Optical transmission T (λ) and (b) I-V graph of the compound VI film.

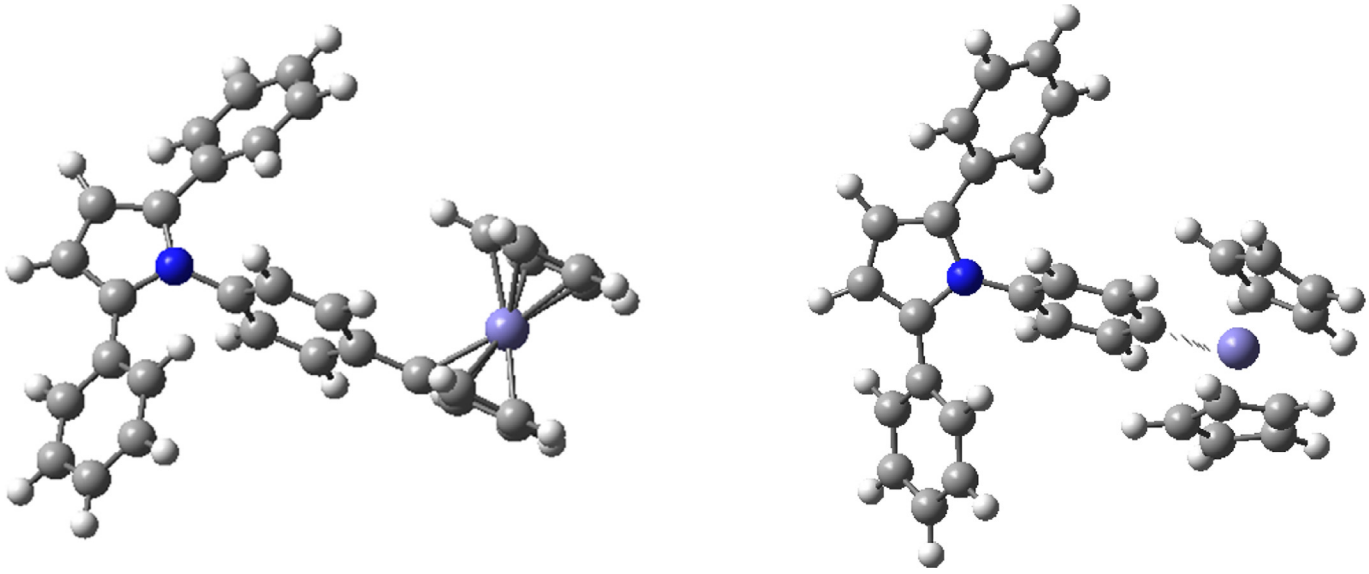

Fig. 11. Optimized structures of the isomers of ferrocene derivatives.

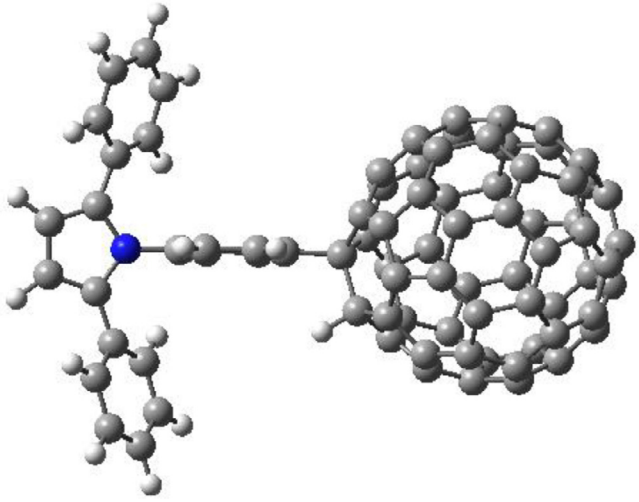

Fig. 12.. Optimized geometry of the fullerene derivative.

sult of 1.97 eV which agree with the Kubelka –Munk result, compound **IV** shows an insulator behaviour because in that case the value is 4.03 eV. With the respect of fullerene derivative **VI** the theoretical result is 1.82 eV which also shows good correlation with the experimental result.

In order to validate the quality of the calculations the geometries of the compounds were compared with published similar cases and we obtain a goodcomparison, for example, the sigma bond between the iron atom and carbon in compound **V** has a bond length of 2.1 Å which corresponds well with other reported compounds of this kind [53].

6. Conclusions

The synthesis of diazonium salts method has been applied successfully to functionalize fullerene and ferrocene molecules, with the known 2, 5-disubstituted pyrrole. The reaction of ferrocene with 2, 5- diphenylpyrrole gives place to two new species, one which entails the formation of a C-C bond and the other with an uncommon Fe-C σ bond, which manifests paramagnetic behaviour. The reaction with fullerene makes it possible to create a fullerene species with a C-C bond, which using a SEM, shows a globular

conformation, characteristic of fullerene derivatives. The Kubelka – Munk analysis and the DFT study show that these three new compounds manifest semiconductor behaviour. The values of E_g obtained for each compound fall within the organic semiconductor range (2-2.9 eV). The fullerene derivative has the lowest E_g value, making it possible to enhance its charge carrying capacity in the pyrrole disubstituted molecule. Likewise, we characterized the film of this compound. Based on the results obtained from the *I-V* analysis, it appears that this semiconductor can be used as a resistor.

Credit author statement

The preparation of precursors and new substances was carried out by GAVH, RDC and LF. The characterization and lab measurements were carried out by VGV, BM, AA and CR. The semiconductor behavior studies were achieved by MESV and RS. The theoretical calculations were carried out by RS and CR. The writing and drawing was carried out by GAVH, LF, MESV, CR and RS.

Declaration of Competing Interest

The authors Giovanna-Angélica Vázquez-Hernández, Roxana Delgado-Cruz, María Elena Sánchez-Vergara, Lioudmila Fomina, Virginia Gómez-Vidales, Beatriz de la Mora, Alonso Acosta, Citlalli Rios, and Roberto Salcedo declare no conflict of interest.

Acknowledgments

Thanks are due to Gerardo Cedillo and Miguel Angel Canseco for their assistance with Nuclear Magnetic Resonance and IR analysis, respectively. The authors wish to express their gratitude to Karla Eriseth Reyes Morales, Omar Novelo Peralta, Adriana Tejeda Cruz and Josué Esaú Romero Ibarra for technical assistance and support in thermal analysis, SEM analysis, DRX analysis and TEM analysis, respectively. We would also like to thank Oralia L Jiménez A., María Teresa Vázquez, Alejandro Pompa, Alberto López-Vivas and Caín González for their technical support. Giovanna Angélica Vázquez-Hernández is grateful for the fellowship and for support from CONACyT.

References

[1] W. Shockley, G.L. Pearson, Modulation of conductance of thin films of semiconductors by surface charges, Phys. Rev. 74 (1948) 232–233.
[2] J. Bardeen, W.H. Brattain, Physical principles involved in transistor action, *Bell. Syst. Tech. J.* 28 (1949) 239–277.
[3] H. Akamatu, H. Inokuchi, On the electrical conductivity of violantrhone, isoviolantrhone and pyranthrone, J. Chem. Phys. 18 (1950) 810–811.
[4] J.H. Burroughes, D.D.C. Bradley, A.R. Brown, R.N. Marks, R.H. Friend, P.L. Burn, A.B. Holmes, Light-emitting-diodes based on conjugated polymers, Nature 347 (1990) 539–541.
[5] J.L. Bredas, D. Beljone, V. Coropceanu, J. Cornil, Charge-transfer and energy–transfer process in π-conjugated oligomers and polymers: a molecular picture, Chem. Rev. 104 (2004) 4971–5003.
[6] H. Hoppe, N.S. Sariciftci, Organic solar cells. An overview, J. Mat. Res. 19 (2004) 1924–1945.
[7] H. Kaur, S. Sundriyal, V. Pachauri, S. Ingebrandt, K.H. Kim, A.L. Sharma, A. Deep, Luminescent metal-organic framework and their composites: potential future materials for light emitting displays, Coord. Chem. Rev. 401 (2019) Art. No. UNSP213077.
[8] H. Bronstein, C.B. Nielsen, B.C. Schroeder, I. McCulloch, The role of chemical design in the performance of organic semiconductors, Nat. Rev. Chem. (2020), doi:10.1038/s41570-019-0152-9.
[9] H. Kleeman, K. Krechan, A. Fischer, K. Leo, A review of vertical organic transistors, Adv. Funct. Mat. (2020) 113 Art. No. 1907.
[10] H. Dong, H. Zhu, Q. Meng, X. Gong, W. Hu, Organic photoresponse materials and devices, Chem. Soc. Rev. 41 (2012) 1754–1808.
[11] S. Nešpůrek, V. Cimrová, J. Pfleger, I. Kminek, Free charge carrier formation in polymers under illumination, Polym. Adv. Technol. 7 (1996) 459–470.
[12] J. Pfleger, S. Kminek, Nešpůrek, W. Schnabel, Electronic transport in poly(methylphenylsilylene) modified by pi-conjugated chromophores, IEEE Trans. Electr. Insul. 27 (1992) 856–860.
[13] Y. Qiao, J. Zhang, W. Xu, D. Zhu, Incorporation of pyrrole to oligothiophene-based quinoids endcapped with dicyanomethylene: a new class of solution processable n-chanel organic semiconductors for air-stable organic field–effect transistors, J. Mat. Chem. 22 (2012) 5706–5714.
[14] A. Facchetti, L. Beverina, M.E. van der Boom, P. Dutta, G. Evmenenko, A.D. Shukla, C.E. Stern, G.A. Pagani, T.J. Marks, Strategies for electrooptic film fabrication. Influence of Pyrrol-Pyridine-based dibranched chromophore architecture on covalent self-assembly, thin film microstructure and non-linear optical response, J. Am. Chem. Soc. 128 (2006) 2142–2153.
[15] G. Huerta, L. Fomina, L. Rumsh, M. Zolotukhin, New polymers with N-phenyl pyrrole fragments obtained by chemical modifications of diacetylene containing polymers, Polym. Bull. 57 (2006) 433–443.
[16] O.G. Morales-Saavedra, G. Huerta, R. Ortega-Martínez, L. Fomina, Linear and non-linear optical properties of 2,5-disubstituted pyrroles supported by a catalyst-free SiO_2 sonogel network, J. Non-Cryst. Sol. 353 (2007) 2557–2566.
[17] L. Fomina, G. Zaragoza-Galan, M. Bizarro, J. Godinez-Sánchez, I.P. Zaragoza, R. Salcedo, Semiconductor behaviour of 2, 5-aromatic disubstituted pyrrole, viewed from and experimental and theoretical perspective, Mat. Chem. Phys. 124 (2010) 257–263.
[18] O. Monroy, L. Fomina, M.E. Sánchez-Vergara, R. Gaviño, A. Acosta, J.R. Álvarez-Bada, R. Salcedo, Synthesis, characterization and semiconducting behavior of N,2,5-trisubstituted pyrroles, J. Mol. Struct. 1171 (2018) 45–53.
[19] J.C. Bijleveld, A.P. Zoombelt, S.G.J. Mathijssen, M.M. Wienk, M. Turbiez, D.M. de Leeuw, A.J. Janssen, Poly(diketopyrrolopyrrole-tertiophene) for ambipolar logic and photovoltaics, J. Am. Chem Soc. 131 (2009) 16616–16617.
[20] C.H. Woo, P.M. Beaujuge, T.W. Holcombe, O.P. Lee, J.M.J. Fréchet, Incorporation of furan into low band-gap polymers for efficient solar cells, J. Am. Chem. Soc. 132 (2010) 15547–15549.
[21] J. March, Advanced Organic Chemistry, 4th Ed, J. Wiley and Sons, New York, 1992.
[22] S. Mahouche-Chergui, S. Gam-Derouich, C. Mangeney, M. Chehimi, Aryl diazonium salts: a new class of coupling agents for bonding polymers, biomacromolecules and nanoparticles to surfaces, Chem. Soc. Rev. 40 (2011) 4143–4166.
[23] S. Patai, The Chemistry of Diazonium and Diazo Group. Parts 1 and 2, Wiley, New York, 1978.
[24] L. Bahr, J. Yang, D.V. Kosynkin, M.J. Bronikowsky, R.E. Smalley, J.M. Tour, Functionalization of carbon nanotubes by electrochemical reduction or aryl diazonium salts: a Bucky paper electrode, J. Am. Chem. Soc. 123 (2001) 6536–6542.
[25] J.J. Gooding, Advances in interfacial design for electrochemical biosensors and sensors: aryl diazonium salts for modifying carbon and metal electrodes, Electroanalysis 20 (2008) 573–582.
[26] K. Flavin, M.N. Chaur, L. Echegoyen, S. Giordani, Functionalization of multilayer fullerenes (carbon nano-onions) using diazonium compounds and “click” chemistry, Org. Lett. 12 (2010) 840–843.
[27] J.R. Lomeda, C.D. Doyle, D.V. Kosynkin, W.F. Hwang, J.M. Tour, Diazonium functionalization of surfactant-wrapped chemically converted graphene sheets, J. Am. Chem. Soc. 130 (2008) 16201–16206.
[28] A.A. Mohamed, Z. Salmi, S.A. Dahoumane, A. Mekki, B. Carbonnier, M.M. Chehimi, Functionalization of nanomaterials with aryldiazonium salts, Adv. Colloid Interfac. 225 (2015) 16–36.
[29] A. Thader, B. Mallik, Observation of persistent photoconductivity at room temperature in ferrocene-doped poly (methyl methacrylate) thin films containing chloroform molecules, Solid State Commun 121 (2002) 2159–3164.
[30] T. Daeneke, T.H. Kwon, A.B. Holmes, N.W. Duffy, U. Bach, L. Spiccia, High-efficiency dye-sensitized solar cells with ferrocene-based electrolytes, Nat. Chem. 3 (2011) 211–215.
[31] E.P. Chuhmanov, N.L. Ermolaev, B.N. Plakhutin, S.K. Ignatov, Tris (perfluoroalkyl) germylethynyl derivatives of biphenyl containing ferrocenyl donor group: strucrer, spectra, and photoinduced intramolecular electron transfer, Comput. Theor. Chem. 1123 (2018) 50–60.
[32] Hillard E.A., Vessières A., Jaouen G. (2010) Ferrocene functionalized endocrine modulators as anticancer agents. In: Jaouen G., Metzler-Nolte N. (eds) Medicinal Organometallic Chemistry. Topics in Organometallic Chemistry, vol 32. Springer, Berlin, Heidelberg.
[33] C.S. Allardyce, A. Dorcier, C. Scolaro, P.J. Dyson, Development of organometallic (organo-transition metal) pharmaceuticals, Appl. Organometal. Chem. 19 (2005) 1–10.
[34] E. Xenogiannopoulou, M. Medved, K. Iliopoulos, S. Couris, M.G. Papadopoulos, D. Bonifazi, C. Sooambar, A. Mate-Alonso, M. Prato, Nonlinear optical properties of ferrocene- and porphyrin- [60]fullerene dyads, ChemPhysChem 8 (2007) 1056–1064.
[35] J. Tauc, R. Grigorovici, A. Vancu, Optical properties and electronic structure of amorphous germanium, Phys. Status Solidi B 15 (1966) 627–637.
[36] P. Kubelka, F. Munk, A contribution to the optics of pigments, Z. Technol. Phys. 12 (1931) 593–599.
[37] P. Makula, M. Pacia, W. Macyk, How to correctly determine the band gap energy of modified semiconductor photocatalysts based on UV-Vis spectra, J. Phys. Chem. Lett. 9 (2018) 6814–6817.
[38] A.B. Murphy, Band-gap determination from diffuse reflectance measurements of semiconductors films, and application to the photoelectrochemical water-splitting, Solar Energy Mater. Solar Cells 91 (2007) 1326–1337.
[39] A.D. Becke, Density-functional exchange-energy approximation with correct asymptotic behavior, Phys. Rev. 38 (1988) 3098–3100.
[40] J.P. Perdew, Y. Wang, Accurate and simple analytic representation of the electron-gas correlation energy, Phys. Rev. B 45 (1992) 13244–13249.

[41] M.J. Frisch, G.W. Trucks, H.B. Schlegel, G.E. Scuseria, M.A. Robb, J.R. Cheeseman, G. Scalmani, V. Barone, B. Menucci, G.A. Petersson, H. Nakatsuji, M. Caricato, X. Li, H.P. Hratchian, A.F. Izmaylov, J. Bloino, G. Zheng, J.L. Sonneberg, M. Hada, M. Ehara, K. Toyota, R. Fukuda, J. Hasegawa, M. Ishida, T. Nakajima, Y. Honda, O. Kitao, H. Nakai, T. Vreven, J.A. Montgomery, J.E. Peralta Jr., F. Ogliaro, M. Bearpark, J.J. Heyd, E. Brothers, K.N. Kudin, V.N. Staroverov, R. Kobayashi, J. Normand, K. Raghavachari, A. Rendell, J.C. Burant, S.S. Iyengar, J. Tomasi, M Cossi, N. Rega, J.M. Millam, M. Klene, J.E. Knox, J.B. Cross, V. Bakken, C. Adamo, J. Jaramillo, R. Gomperts, R.E. Stratmann, O. Yazyev, A.J. Austin, R. Cammi, C. Pomelli, J.W. Ochterski, R.L. Martin, K. Morokuma, V.G. Zakrzewski, G.A. Voth, P. Salvador, J.J. Dannenberg, S. Dapprich, A.D. Daniels, Ö. Farkas, J.B. Foresman, J.V. Ortiz, J. Cioslowski, D.J. Fox, Gaussian 09, Revisión A.1, Gaussian, Inc., Wallingford CT, 2009.
[42] C. Glaser, Beiträge zur Kenntniss des Acetenylbenzols, Ber. Dtsh. Chem. Ges 2 (1869) 422–424.
[43] A.S. Hay, Oxidative coupling of acetylenes. II, J. Org, Chem. 27 (1962) 3320–3321.
[44] J. Reisch, K.E. Shulte, Pyrrol-Derivate aus Diacetylenen, Angew. Chemie 73 (1961) 241.
[45] K.E. Schulte, J. Reisch, H. Walker, Eine neue Pyrrolsynthese aus Butadiin-Derivaten, Chem. Ber. 98 (1965) 98–103.
[46] K.E. Schulte, J. Reisch, H. Walker, Dipyrrole und Porphin aus Acetylenverbindungen, Arch. Pharm. 299 (1966) 1–7.
[47] G. Gillies, D. Dönnecke, W. Imhof, How to control the chemioselectivity of the catalytic formation of chiral γ-lactams or 2-3 disubstituted pyrroles by the choice of solvent, Monatshefte für Chemie 138 (2007) 683–686.
[48] A.J. Béchamp, De l' action des protosels de fer sur la nitronapthaline et la nitrobenzine. Nouvelle méthode de formation des bases organiques artificielles de Zinin, Ann. *Chim. Phys.* 42 (1854) 186–196.
[49] P.A. Pasha, V.P. Jayashankara, Sn/NH_4 Br assisted selective reduction of nitroarenes into anilines under neutral conditions, Indian J. Chem. 43B (2004) 2464–2466.
[50] A. Agrawal, P.G. Tratnyek, Reduction or nitro aromatic compounds by zero-valent iron metal, Environ. Sci. Technol. 30 (1996) 153–160.
[51] D. Koziakov, G. Wu, A. Jacobi von Wangelin, Aromatic substitutions of arenediazonium salts via metal catalysis, single electron transfer and weak base mediation, Org. Biomol. Chem. 16 (2018) 4942–4953.
[52] C. Rowlands, D.M. Murphy, in: Chemical Applications of EPR, Handbook of Nuclear Chemistry, Cardiff University, UK, 2006, p. 190.
[53] M.W. Wallasch, D. Weismann, C. Riehn, S. Ambrus, G. Wolmershäuser, A. Lagutschenkov, G. Niedner-Schatteburg, H. Sitzmann, Reactive Sigma-Aryl-iron complexes or iron-promoted coupling of two phenyl anions to one bis(cyclohexadienylidene) ligand: synthesis, structure, mass spectrometry, and DFT calculations, Organometallics 29 (2010) 806–813.
[54] C.P. Chai, Y.P. Wang, R.M. Wang, H.X. Ren, C.J. Hao, Condensation polymers of dicyclopentadienyl iron with aromatic diazonium salts and magnetism, Polym. Adv. Technol. 15 (2004) 55–60.
[55] R. Taylor, The Chemistry of Fullerenes, World Scientific, Singapore, 1995.
[56] A. Hirsch, T. Grösser, A. Skiebe, A. Soi, Synthesis of isomerically pure organohydrofullerenes, Chem. Ber. 126 (1993) 1061–1067.
[57] A. Hirsch, A. Soi, H.R. Karfunkel, Tritation of C60: a method for the synthesis of organofullerenes, Angew. Chem. Ind. Ed. Engl. 31 (1992) 766–768.
[58] G.V. Andrievsky, V.K. Klochov, A.B. Bordyuh, G.I. Dovbeshko, Comparative analysis of two aqueous-colloidal solutions of C_{60}-fullerene with help of FTIR reflectance and UV-Vis spectroscopy, Chem. Phys. Lett. 364 (2002) 8–17.
[59] H.U. Kim, D. Mi, J.H. Kim, J.B. Park, S.C. Yoon, U.C. Yoon, D.H. Hwang, Carbazole -containing fullerene derivatives for P3HT-base bulk-heterojunction solar cells, Solar Energy Mater. Solar Cells 105 (2012) 6–14.
[60] T. Huang, B. Jin, F.R. Peng, C.D. Chen, R.Z. Zheng, Y. He, S.J. Chu, Synthesis and characterization of [60]fullerene-glycidyl azide polymer and its thermal decomposition, Polymers 7 (2015) 896–908.
[61] D.M. Guldi, C. Luo, A. Swartz, R. Gomez, J.L. Segura, N. Martin, C. Brabec, N.S. Sariciftci, Molecular engineering of C60-based conjugated oligomer ensembles: modulating the competition between photoinduced energy and electron transfer processes, J. Org. Chem. 67 (2002) 1141–1152.
[62] A.W. Hains, Z. Liang, M.A. Woodhouse, B.A. Gregg, Molecular semiconductors in organic photovoltaic cells, Chem. Rev. 110 (2010) 6689–6735.
[63] M. Carano, M. Da Ros, M. Fanti, K. Kordatos, M. Marcaccio, F. Paolucci, M. Prato, S. Roffia, F. Zerbetto, Modulation of the reduction potentials of fullerene derivatives, J. Am. Chem. Soc. 125 (23) (2003) 7139–7144.
[64] H. Imahori, S. Fukuzumi, Porphyrin and fullerene-based molecular photovoltaic devices, Adv. Funct. Mater. 14 (2004) 525–536.
[65] M.M. Wienk, J.M. Kroon, W.J.H. Verhees, J. Knol, J.C. Hummelen, P.A. van Hal, R.A.J. Janssen, Efficient methanol [70]fullerene/MDMO-PPV bulk heterojunction photovoltaics cells, Angew Chem. Int. Ed. Engl. 42 (2003) 3371–3375.
[66] J. Labille, A. Masion, F. Ziarelli, J. Rose, J. Brant, F. Villiéras, M. Pelletier, D. Borschneck, M.R. Wiesner, Y. Bottero, Hydration and dispersion of C60 in aqueous systems: the nature of water-fullerene interactions, Langmuir 25 (2009) 11232–11235.
[67] A. Hazanzadeh, A. Khataee, M. Zarei, Y. Zhang, Two-electron oxygen reduction on fullerene C60-carbon nanotubes covalent hybrid as a metal-free electrocatalyst, Sci. Rep. 9 (2019) 13780.
[68] Dongbo D. Mi, DoD.-Hoon H. Hwang, Synthesis and characterization of novel soluble fulleropyrrolidine derivatives and their photovoltaic performance, J. Nanosci. Nanotechnol. 13 (2013) 3474–3479.